SCIENTIFIC REPORTS

OPEN

SUBJECT AREAS:
PLANT SCIENCES
MUTATION
PHENOTYPE
INNATE IMMUNITY

Received
13 October 2011

Accepted
9 November 2011

Published
25 November 2011

Correspondence and requests for materials should be addressed to A.I. (ishikawa@fpu.ac.jp)

Non-host resistance to penetration and hyphal growth of *Magnaporthe oryzae* in *Arabidopsis*

Misato Nakao, Ryotaro Nakamura, Kaori Kita, Ryuya Inukai & Atsushi Ishikawa

Department of Bioscience, Fukui Prefectural University, Fukui, 910–1195, Japan.

Rice blast caused by *Magnaporthe oryzae* is a devastating disease of rice. Mechanisms of rice resistance to blast have been studied extensively, and the rice–*M. oryzae* pathosystem has become a model for plant–microbe interaction studies. However, the mechanisms of non-host resistance (NHR) to rice blast in other plants remain poorly understood. We found that penetration resistance to *M. oryzae* in multiple mutants, including *pen2 NahG pmr5 agb1* and *pen2 NahG pmr5 mlo2* plants, was severely compromised and that fungal growth was permitted in penetrated epidermal cells. Furthermore, rice Pi21 enhanced movement of infection hyphae from penetrated *Arabidopsis* epidermal cells to adjacent mesophyll cells. These results indicate that PEN2, PMR5, AGB1, and MLO2 function in both penetration and post-penetration resistance to *M. oryzae* in *Arabidopsis*, and suggest that the absence of rice Pi21 contributed to *Arabidopsis* NHR to *M. oryzae*.

Rice is a staple crop of economic importance in many countries. One of the most serious and widespread rice diseases is blast, which is caused by the ascomycete fungus *Magnaporthe oryzae*. The mechanisms underlying rice resistance to blast have been studied extensively, and the rice–*M. oryzae* pathosystem has become a model for the study of plant–microbe interactions because both whole genome sequences and functional genomic approaches are available[1–5]. The infection of rice by *M. oryzae* follows a developmental process that occurs in many foliar fungal pathogens. A germ tube produced from the conidium differentiates into a specialized infectious structure called the appressorium, which adheres tightly to the plant surface with mucilage. The fungus generates massive turgor pressure inside the melanized appressorium, forcing a narrow penetration peg through the host surface and allowing the entry of the fungus into a leaf epidermal cell[6]. After penetration, the peg differentiates into bulbous and lobed infectious hyphae that grow intra- and intercellularly.

Most plants are immune to the majority of potential pathogens, and are susceptible to only a few adapted microbes. Consequently, disease is the exception rather than the rule. Disease resistance in all members of a plant species to all genetic variants of a non-adapted pathogen species is the most common form of plant immunity, which is termed non-host resistance (NHR)[7,8]. Although NHR represents the most common and durable form of plant resistance in nature, it is poorly understood at the molecular level.

Arabidopsis mutants with altered non-host interactions following *Blumeria graminis hordei* (*Bgh*) infection were described recently, and three genes were identified: *PENETRATION 1* (*PEN1*), *PEN2*, and *PEN3*[9–12]. *PEN1* encodes a plasma membrane–anchored syntaxin with a soluble N-ethylmaleimide-sensitive factor attachment protein receptor (SNARE) domain[9]. *PEN2* encodes an atypical myrosinase involved in glucosinolate metabolism in defense responses[10,13,14]. *PEN3* encodes a pleiotropic drug resistance (PDR) ATP-binding cassette (ABC) transporter[11,12]. Collectively, these studies demonstrate that *Arabidopsis* NHR to non-adapted biotrophic powdery mildews has two successive and multicomponent defense layers: pre- and post-invasion resistance. Notably, PEN2 and PEN3 contribute to both stages of resistance[10,11]. Moreover, enhanced disease susceptibility 1 (EDS1), phytoalexin-deficient 4 (PAD4), and senescence-associated gene 101 (SAG101) are factors in post-invasion resistance[10].

The *Arabidopsis pen2* mutant also shows a significantly elevated *M. oryzae* penetration ratio[15–17]. Furthermore, PMR5 and AGB1 are positive regulator factors for penetration resistance in the *Arabidopsis–M. oryzae* interaction[15]. Broad-spectrum resistance to adapted powdery mildews is conferred by loss-of-function mutant alleles of *MILDEW RESISTANCE LOCUS O* (*MLO*) genes in barley and *Arabidopsis*. *MLO* encodes a plant-specific family of integral membrane proteins. Barley plants carrying a mutation in the *MLO* locus, which confers a durable resistance to powdery mildew, are hypersusceptible to the rice blast fungus *Magnaporthe oryzae*[18]. Rice

pi21 is a recessive gene conferring durable resistance to blast disease; it encodes a loss-of-function mutation in a cytoplasmic proline-rich protein consisting of a putative heavy metal–binding domain and putative protein–protein interaction motifs. The rate of hyphae penetration from penetrated cells into adjacent cells, which is an indicator of hyphal growth, is significantly lower in *pi21* plants than in *Pi21* plants, suggesting that the susceptible *Pi21* allele negatively regulates resistance[19]. Despite the identification of these factors, their roles in NHR to *M. oryzae* are unknown.

Here, we report the NHR genetic interactions revealed by our examination of the mechanisms operating in *Arabidopsis*. We found PEN2, PMR5, AGB1, and MLO2 to be involved in several steps of NHR to *M. oryzae*. Moreover, we demonstrated that rice Pi21 enhanced movement of *M. oryzae* infection hyphae from penetrated *Arabidopsis* epidermal cells to adjacent mesophyll cells.

Results

The roles of PMR5 and AGB1 in *Arabidopsis* NHR to *M. oryzae*. We recently demonstrated that PMR5 and AGB1 contributed to *Arabidopsis* resistance to penetration by *M. oryzae*, indicating that a genetic network regulated this resistance[15]. In the present study of the genetic network, we generated *pen2 NahG pmr5*, *pen2 NahG agb1*, *pen2 pmr5 agb1*, and *pen2 NahG pmr5 agb1* mutants. We performed an experiment to compare *M. oryzae* entry rates among different *Arabidopsis* mutants. Around 24 h post-inoculation (hpi), *M. oryzae* penetrated *Arabidopsis* epidermal cells; we harvested leaves of infected plants at 26 and 48 hpi and examined them microscopically. Consistent with our previous observations, entry rates into *pen2 NahG*, *pen2 pmr5*, and *pen2 agb1* double mutants were higher than the rate into *pen2* mutants (Fig. 1a)[15]. The triple mutants (*pen2 NahG pmr5*, *pen2 NahG agb1*, and *pen2 pmr5 agb1*) had higher rice blast entry rates than the *pen2* double mutants (Fig. 1a). Moreover, the entry rate was significantly increased ($P < 0.05$) into the *pen2 NahG pmr5 agb1* mutant as compared with the other mutants (Fig. 1a). Entry rates into these mutants at 48 hpi were usually higher than those at 26 hpi, indicating that penetration continued up to 48 hpi (Fig. 1a and Supplementary Fig. S1a). We estimated the penetration ratio of multiple mutants by summing the frequencies of individual mutants and showed that *NahG*, *pmr5*, and *agb1* may have additive effects on *Arabidopsis* penetration resistance to *M. oryzae*.

Previously, we reported that *M. oryzae* penetrated epidermal cells, but showed no further intra- or intercellular growth in *Arabidopsis pen2 NahG*, *pen2 pmr5*, and *pen2 agb1* mutants[15]; we concluded that PMR5 and AGB1 contributed only to penetration resistance. However, during microscopic examination of *pen2 NahG pmr5 agb1* mutants in the present study, we noticed that infection hyphae in the plants were longer (≥30 μm) than in the *pen2* mutant (<ca. 10 μm), and some of them had branched by 48 hpi (Fig. 1b–g). Accordingly, we measured the lengths of the longest infection hyphae in these multiple mutants at 26 and 48 hpi. The longest infection hyphae in *pen2 NahG*, *pen2 pmr5*, and *pen2 agb1* double mutants were longer than those in the *pen2* mutant at 26 and 48 hpi (Fig. 1b and Supplementary Fig. S1b). Infection hypha in the triple mutants (*pen2 NahG pmr5*, *pen2 NahG agb1*, and *pen2 pmr5 agb1*) were longer yet than those in *pen2* double mutants at 26 and 48 hpi (Fig. 1b and Supplementary Fig. S1b). Furthermore, infection hypha length in the *pen2 NahG pmr5 agb1* mutant was significantly ($P < 0.05$) greater than lengths in *pen2* double mutants at 26 and 48 hpi (Fig. 1b and Supplementary Fig. S1b). Infection hypha lengths in these multiple mutants increased between 26 and 48 hpi, except in *pen2* and *pen2 NahG* plants, indicating that elongation of infection hyphae continued through 48 hpi in most of the mutants (Fig. 1b and Supplementary Fig. S1b). We found that infection hypha lengths in these multiple mutants could be roughly estimated by summing the lengths in individual mutants. Hence, *NahG*, *pmr5*, and *agb1* may have additive effects on fungal elongation in *Arabidopsis* tissues.

We evaluated *M. oryzae* penetration success through the occurrence of autofluorescence at infection sites; the autofluorescence we observed resulted from hypersensitive responses resembling cell death that were triggered by penetration. Hence, the penetration process included not only the breaching of epidermal cell walls, but also hyphal elongation in penetrated cells that induced cell death. Therefore, we examined the penetration process by using higher-magnification microscopy to classify *Arabidopsis* defense responses. We were readily able to divide the process into four events (I–IV): (I) cell wall penetration, (II) establishment of infection hyphae, (III) elongation of infection hyphae, and (IV) branch formation on infection hyphae (Fig. 1c). No visible infection hyphae (Fig. 1d) were detected in about 30% of penetrated *pen2* epidermal cells, short (<10 μm) infection hyphae (Fig. 1e) developed in about 40% of penetrated cells, long (>10 μm) infection hyphae (Fig. 1f) developed in about 25%, and branched hyphae (Fig. 1g) developed in <5% of penetrated cells. Thus, the PEN2-mediated pathway likely controlled not only cell wall penetration, but also the establishment of *M. oryzae* infection hyphae in penetrated epidermal cells.

We subsequently examined the penetration process in *pen2* double mutants (*pen2 NahG*, *pen2 pmr5*, and *pen2 agb1*) under high magnification. Among these mutants, no visible infection developed in ~10% of penetrated cells; this proportion differed significantly from that in *pen2* plants ($P < 0.05$; Fig. 1d). These double mutants produced short (<10 μm) infection hyphae in approximately 25% of penetrated cells (Fig. 1e). The *pen2 pmr5* and *pen2 agb1* mutants had significantly higher proportions of long (>10 μm) infection hypha development ($P < 0.05$) as compared with *pen2* mutants (Fig. 1f). Notably, long infection hyphae developed in >50% of penetrated cells in *pen2 pmr5* plants (Fig. 1f). Branched hyphae developed in only about 10% of penetrated cells in *pen2 pmr5* plants; the proportions of penetrated cells (~20%) in *pen2 NahG* and *pen2 agb1* mutants that developed branched hyphae were significantly higher than that in the *pen2* mutant ($P < 0.05$; Fig. 1g).

We further examined the penetration process in *pen2 NahG pmr5*, *pen2 NahG agb1, pen2 pmr5 agb1*, and *pen2 NahG pmr5 agb1* mutants. Among these *pen2* multiple mutants, visible infection hyphae developed in >90% of penetrated cells; this proportion differed significantly from that in *pen2* plants ($P < 0.05$; Fig. 1d). Short (<10 μm) infection hyphae were produced in these multiple mutants (with the exception of *pen2 pmr5 agb1* plants) much less frequently than in the *pen2* double mutants (Fig. 1e). The *pen2 NahG pmr5 agb1* plants had especially reduced proportions of this fungal phenotype ($P < 0.05$; Fig. 1e). The proportions of long (>10 μm) infection hyphae in these multiple mutants did not differ markedly from those in *pen2* double mutants (Fig. 1f) after penetration. The proportion of branched hyphae formed in *pen2 NahG agb1* plants equaled the sum of the proportions in *pen2 NahG* and *pen2 agb1* plants, indicating that the effects of *NahG* and *agb1* on branch formation were additive (Fig. 1g). Although we detected no effect of *pmr5* in *pen2 NahG pmr5* and *pen2 pmr5 agb1* plants in our comparison with *pen2 NahG* and *pen2 agb1* plants, *pen2 NahG pmr5 agb1* plants had significantly higher proportions of branched hyphae than any other genotype ($P < 0.05$; Fig. 1g).

The role of MLO2 in *Arabidopsis* NHR to *M. oryzae*. Previously, we showed that MLO2 had no NHR function in *Arabidopsis–M. oryzae* interactions[15]. However, barley plants carrying a mutation in the *MLO* locus, which confers durable resistance to powdery mildew, are hypersusceptible to the rice blast fungus *Magnaporthe oryzae*[18]. Therefore, we continued analysis of the *mlo* mutation in different genetic backgrounds to determine the NHR *MLO* function in *Arabidopsis–M. oryzae* interactions. To identify the role of MLO2 in NHR, we generated *pen2 NahG mlo2*, *pen2 pmr5 mlo2*, and *pen2*

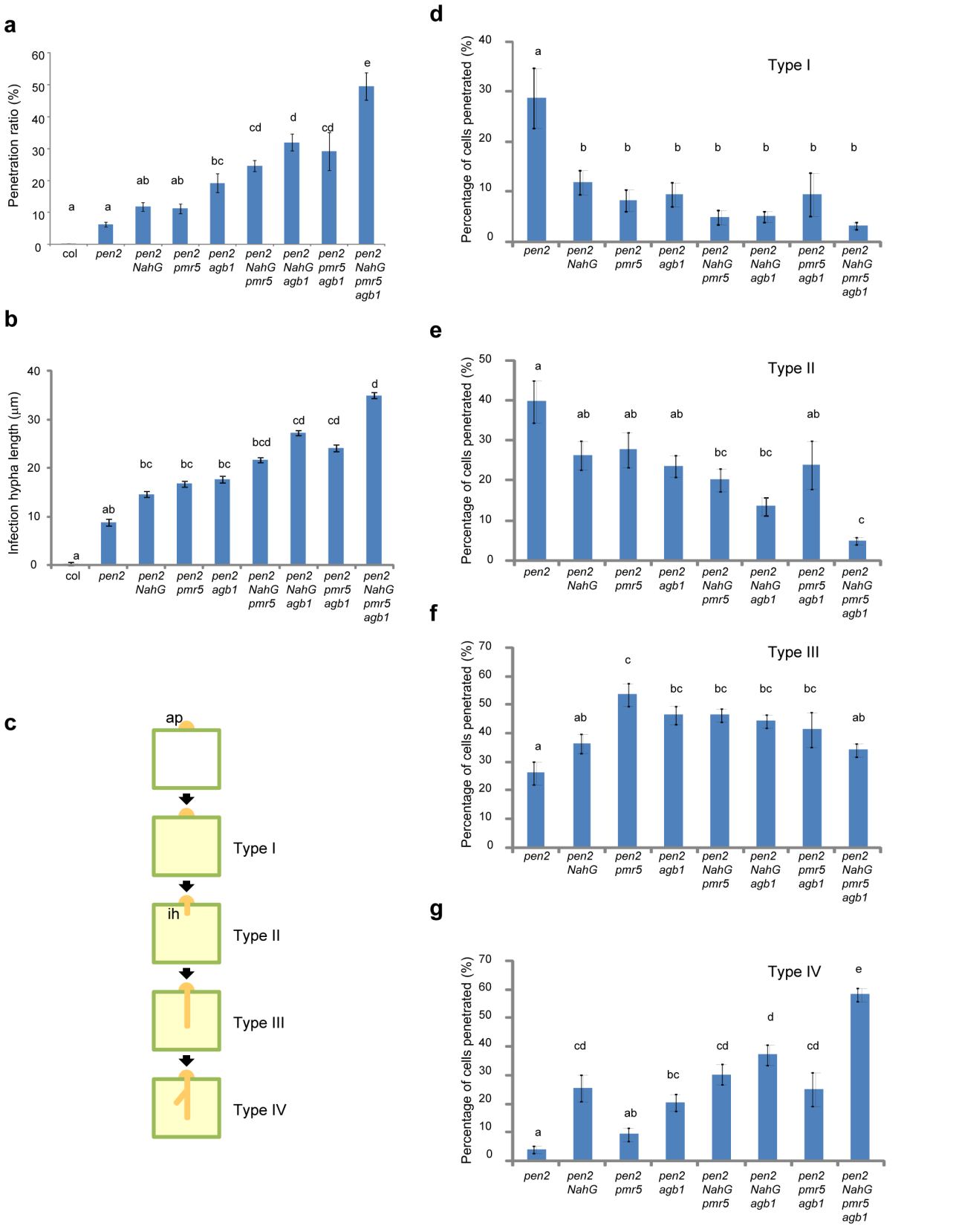

Figure 1 | Quantitative analysis of *Arabidopsis* mutant non-host resistance to *M. oryzae*. (a) Mean frequency of *M. oryzae* penetration into *Arabidopsis* mutants 48 h post-inoculation (hpi) expressed as a percentage of total infection sites. (b) Mean length of infection hyphae was measured at 48 hpi. (c) The penetration process was divided into four events (I–IV): I, successful penetration without infection hyphae; II, successful penetration with short (<10 μm) infection hyphae; III, successful penetration with long (>10 μm) infection hyphae; and IV, successful penetration with branched hyphae. The epidermal cells penetrated accumulated autofluorescent compounds (pale yellow). ap, appressorium, ih, infection hypha. (d–g) Mean frequencies of infection site types on *Arabidopsis* mutants at 48 hpi, expressed as percentages of penetrated cells. (d) Type I, (e) type II, (f) type III, (g) type IV. Values are means ± standard errors ($n = 3$). Bars sharing the same lowercase letters are not significantly different (Tukey's highly significant difference test; $P \geq 0.05$; $n = 3$).

NahG pmr5 mlo2 plants and performed an experiment to compare *M. oryzae* entry rates into these mutants. We harvested leaves of infected plants at 26 and 48 hpi and examined them microscopically. Consistent with our previous observations, entry rates into *pen2 mlo2* plants did not differ from that into the *pen2* mutant (Fig. 2a)[15]. The entry rate into *pen2 NahG mlo2* plants was higher than the rate into *pen2* double mutants and equal to the sum of entry rates into *pen2 NahG* and *pen2 mlo2* plants (Fig. 2a). Thus, *mlo2* had an additive effect on penetration resistance in the *pen2 NahG* genetic background. Moreover, *pen2 pmr5 mlo2* plants had significantly higher penetration rates than *pen2* double mutants ($P < 0.05$; Fig. 2a); *pen2 NahG pmr5 mlo2* plants also had significantly higher penetration rates than other mutants ($P < 0.05$; Fig. 2a), indicating that *mlo2* likely had synergistic effects on penetration resistance in the *pen2 pmr5* genetic background. Based on these data, we suggest that *mlo2* and *NahG* acted independently, and that *mlo2* and *pmr5* acted synergistically in their effects on *Arabidopsis* penetration resistance against *M. oryzae*.

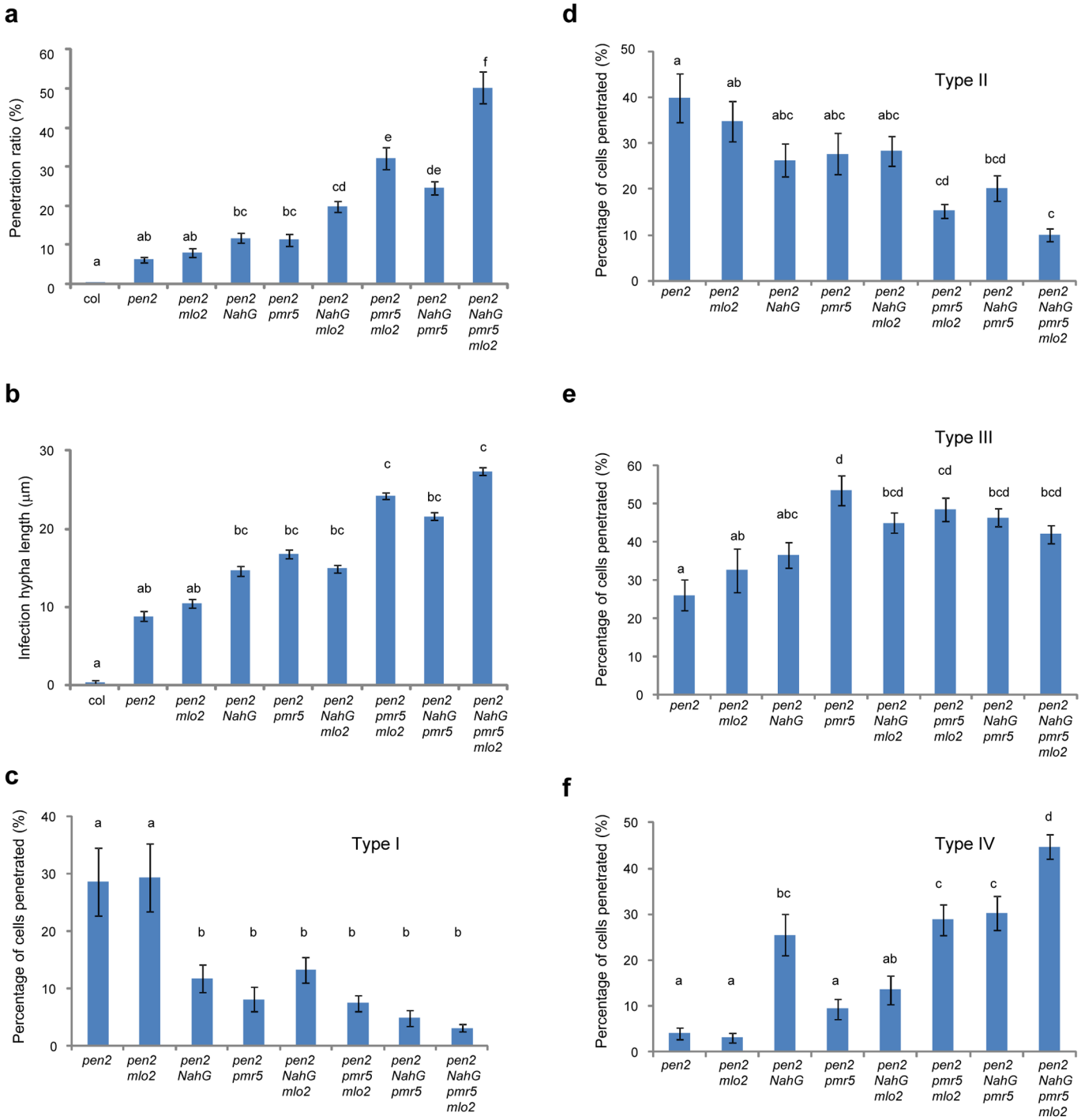

Figure 2 | Quantitative analysis of *mlo2* multiple mutant *Arabidopsis* non-host resistance to *M. oryzae*. (a) Mean frequencies of *M. oryzae* penetration in *Arabidopsis* mutants at 48 h post-inoculation (hpi) expressed as percentages of total infection sites. (b) Mean lengths of infection hypha measured at 48 hpi. (c–f) Mean frequencies of infection site types in *Arabidopsis* mutants at 48 hpi expressed as percentages of penetrated cells. (c) Type I, (d) type II, (e) type III, (f) type IV. Values are means ± standard errors ($n = 3$). Bars sharing the same lowercase letters are not significantly different (Tukey's highly significant differences test; $P \geq 0.05$, $n = 3$).

We further investigated the role of MLO2 in post-penetration resistance by measuring lengths of the longest infection hyphae in *mlo* mutants at 26 and 48 hpi (Fig. 2b and Supplementary Fig. S2b). The lengths of infection hyphae in the *pen2 mlo2* double mutant and *pen2* mutant did not differ (Fig. 2b). The lengths of infection hyphae in *pen2 NahG mlo2* plants and *pen2 NahG* double mutants also did not differ (Fig. 2b). However, the infection hyphae in *pen2 pmr5 mlo2* and *pen2 NahG pmr5 mlo2* plants were longer than those in control plants (Fig. 2b). Thus, the effect of *mlo2* was likely expressed only in the *pen2 pmr5* genetic background and MLO2 likely played a role in post-penetration resistance.

Subsequently, we examined the penetration process in the *pen2 mlo2* double mutant under high magnification. The distribution of cellular reaction types in the *pen2 mlo2* and *pen2* mutants did not differ (Fig. 2c–f). We also examined hyphal penetration in *pen2 NahG mlo2*, *pen2 pmr5 mlo2*, and *pen2 NahG pmr5 mlo2* plants. Among these, visible infection hyphae developed in more than ~90% of penetrated cells, a proportion that differed significantly from that in *pen2 mlo2* plants ($P < 0.05$; Fig. 2c). Short (<10 μm) infection hyphae were produced much less frequently in these multiple mutants (except for *pen2 NahG mlo2* plants) than in *pen2 mlo2* plants (Fig. 2d). Proportions of penetrated cells that developed long (>10 μm) infection hyphae did not differ between *pen2 pmr5 mlo2* and *pen2 pmr5* plants (Fig. 2e). The proportion of penetrated cells that developed branched hyphae in *pen2 NahG mlo2* was intermediate between proportions in *pen2 mlo2* and *pen2 NahG* plants. The branched hyphal development proportion in *pen2 pmr5 mlo2* plants was significantly ($P < 0.05$) higher than those in *pen2 mlo2* and *pen2 pmr5* plants (Fig. 2f); the proportion in *pen2 NahG pmr5 mlo2* plants was significantly higher than that in *pen2 NahG pmr5* plants ($P < 0.05$; Fig. 2f). These data indicate that *mlo2* likely had a synergistic effect on the formation of branched hyphae in the *pen2 pmr5* genetic background.

Rice Pi21 enhances hyphal growth of *M. oryzae* in *Arabidopsis*. The *pen2 NahG pmr5 agb1* and *pen2 NahG pmr5 mlo2 Arabidopsis* plants had the highest rates of hyphal penetration (Figs. 1a, 2a and Supplementary Figs. S1a, S2a), longest hyphae (Figs. 1b, 2b and Supplementary Figs. S1b, S2b), highest proportions of branched hypha formation (Figs. 1g and 2f), and highest proportions of hyphal growth from penetrated cells to adjacent cells (Supplementary Fig. S3); however, they prevented *M. oryzae* from completing its life cycle to form asexual conidia. Hence, unidentified genes in *Arabidopsis* probably control post-penetration resistance to *M. oryzae*. Alternatively, essential factors needed to establish the rice blast infection may be absent in *Arabidopsis*, in which case, these factors should be present in rice. Rice blast susceptibility factor Pi21 may function in this role.

To test whether rice *Pi21* affected *Arabidopsis* NHR to *M. oryzae*, we generated transgenic lines in *pen2*, *pen2 NahG pmr5 agb1,* and *pen2 NahG pmr5 mlo2* genetic backgrounds, expressing rice *Pi21* under the control of a 35S promoter. Although we were able to generate sufficient numbers of transgenic *Pi21* lines in *pen2* and *pen2 NahG pmr5 mlo2* backgrounds (Fig. 3a and Supplementary Fig. S4), we were not able to produce sufficient numbers in the *pen2 NahG pmr5 agb1* background to permit further study. Our analysis was therefore restricted to two genetic backgrounds.

We first examined *M. oryzae* entry rates in these transgenic *Pi21* lines. Leaves of infected plants were harvested at 48 hpi and inspected microscopically. Entry rates into transgenic *Pi21* lines did not differ among *pen2 and pen2 NahG pmr5 agb1* backgrounds and control plants (Fig. 3b and Supplementary Fig. S5a). Subsequently, we measured the lengths of the longest infection hyphae in these transgenic lines at 48 hpi. The lengths of the infection hyphae did not differ between transgenic lines in the *pen2* background and *pen2* plants (Supplementary Fig. S5b); however, the lengths of infection hyphae in transgenic lines in the *pen2 NahG pmr5 mlo2* background were significantly greater than those in control *pen2 NahG pmr5 mlo2* plants ($P < 0.05$; Fig. 3c).

We further examined the penetration process in transgenic *Pi21* lines by high-magnification microscopy. The distribution of cellular reaction types did not differ between transgenic lines in *pen2* and *pen2 NahG pmr5 mlo2* backgrounds and control plants (Fig. 3d–g and Supplementary Fig. S6).

We also examined the movement of fungal hyphae in transgenic lines from penetrated epidermal cells to adjacent epidermal or mesophyll cells. The movement phenotypes were grouped as follows: (A) movement to adjacent epidermal cell (Fig. 4a, b), (B) movement to adjacent mesophyll cell (Fig. 4c, d), and (C) movement to adjacent epidermal and mesophyll cells. Significantly higher rates of hyphal movement from penetrated cells into adjacent mesophyll cells were observed in transgenic *Pi21* lines in the *pen2 NahG pmr5 mlo2* background ($P < 0.05$); however, this was not the case for movement into adjacent epidermal cells (Fig. 4e–g). This *Arabidopsis* phenotype resembled transgenic rice plants expressing *Pi21*[19]. However, no hyphal movement was observed in *Arabidopsis* transgenic lines expressing *Pi21* in the *pen2* background (Supplementary Fig. S7), indicating that *NahG, pmr5,* and *mlo2* mutations are likely necessary factors allowing *Pi21* to function in the *pen2 Arabidopsis* mutant.

Discussion

Our systematic analyses of multiple mutant combinations revealed the genetic network of penetration and post-penetration resistance to *M. oryzae* in *Arabidopsis*. In multiple mutants, including *pen2 NahG pmr5 agb1* and *pen2 NahG pmr5 mlo2* plants, penetration resistance to *M. oryzae* was severely compromised, and fungal growth in penetrated epidermal cells was also greater than in the *pen2* mutant (Figs. 1, 2 and Supplementary Figs. S1, S2). Thus, PEN2, PMR5, AGB1, and MLO2 were likely involved in *Arabidopsis* penetration and post-penetration resistance to *M. oryzae*. Moreover, *Arabidopsis* transgenic lines expressing rice *Pi21* in the *pen2 NahG pmr5 mlo2* background permitted fungal cell–cell movement (Fig. 4), suggesting that the absence of rice susceptibility to the *M. oryzae* gene *Pi21* may contribute to *Arabidopsis* NHR.

Transgenic *NahG* plants and the *pmr5*, *agb1*, and *mlo2* single mutants did not support fungal penetration success and hyphal elongation in *M. oryzae–Arabidopsis* interactions[15]; however, the entry rates into *pen2 NahG*, *pen2 pmr5*, and *pen2 agb1* plants exceeded those into the *pen2* mutant[15]. The penetration ratio of *pen2 pmr5 agb1* plants was obtained by summing the frequencies for individual mutants (Figs. 1a and 2a), suggesting that *pmr5* and *agb1* have additive effects on the rates in the *pen2* background. Hence, PMR5 and AGB1 probably acted independently in *Arabidopsis* penetration resistance to *M. oryzae*. In our previous study, the *pen2* and *pen2 mlo2* mutants did not differ in penetration resistance to rice blast[15]. However, in the present work, *mlo2* had both an additive effect on hyphal penetration rates in the *pen2 NahG* background (Fig. 2a) and a synergistic effect on these rates in the *pen2 pmr5* background (Fig. 2a). Hence, MLO2 and NahG probably acted independently, and MLO2 and PMR5 likely acted synergistically, in *Arabidopsis* rice blast penetration resistance.

Because we detected no difference in post-penetration resistance among *pen2*, *pen2 NahG*, *pen2 pmr5*, and *pen2 agb1* plants in our previous study, we concluded that PMR5 and AGB1 were not involved in post-penetration resistance[15]. However, in the present investigation, we found that frequencies of long (>10 μm) infection hyphae in *pen2 pmr5* and *pen2 agb1* plants were significantly ($P < 0.05$) higher than those in *pen2* plants (Fig. 1f). Further, rates of infection hypha branch formation were significantly higher in *pen2 NahG* and *pen2 agb1* plants than in *pen2* plants (Fig. 1g). Hence, PMR5 functioned mainly in the inhibition of hyphal elongation following fungal penetration in the *pen2* genetic background. NahG

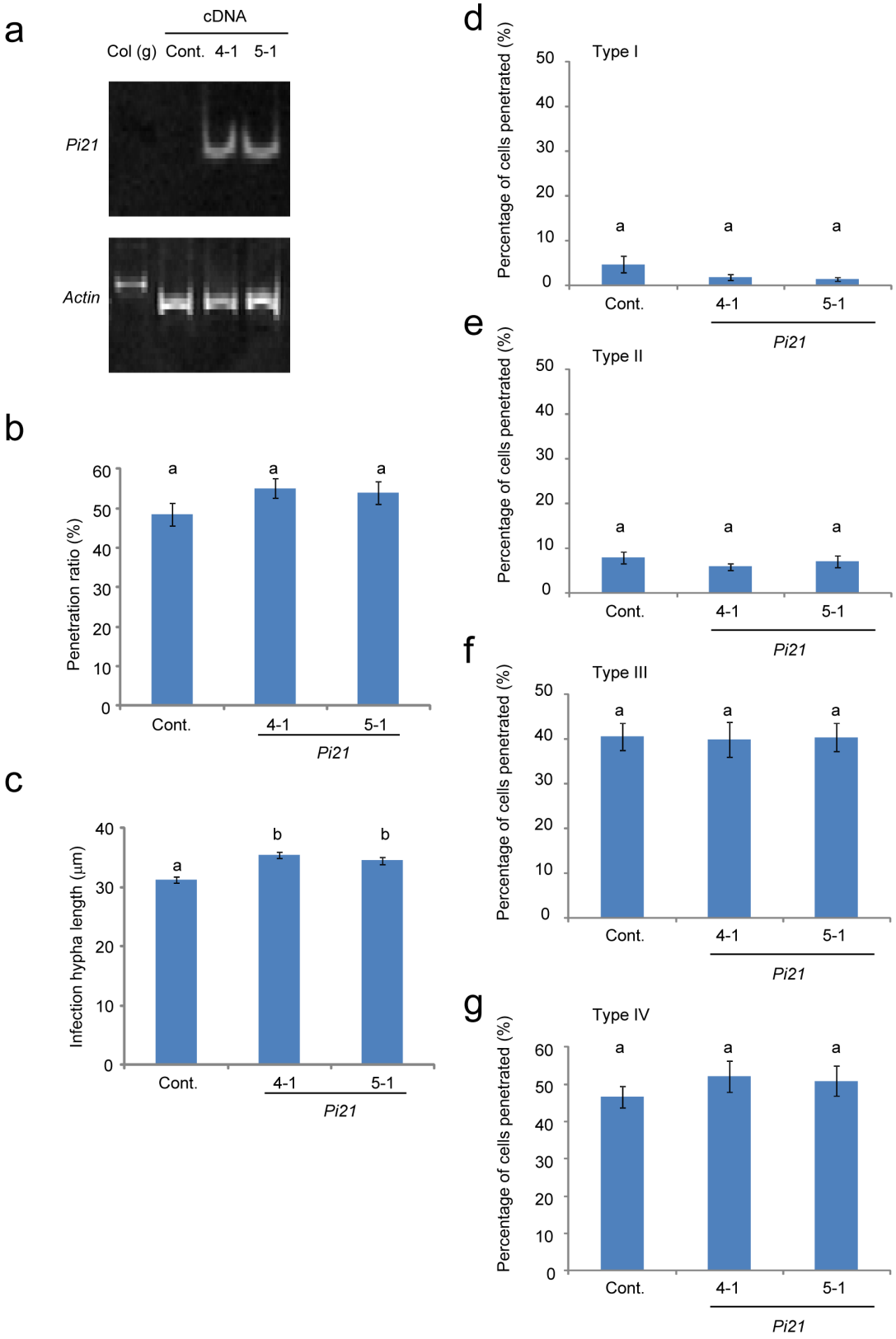

Figure 3 | Characterization of transgenic *Arabidopsis Pi21* lines. (a) Reverse transcription polymerase chain reaction (RT-PCR) analysis of *Pi21* in transgenic *Arabidopsis Pi21* lines (*pen2 NahG pmr5 mlo2* background). Col (g), genomic DNA of *Arabidopsis* accession Col-0 served as a control template for distinguishing cDNA and genomic DNA–derived PCR products. (b) Mean frequencies of *M. oryzae* penetration in transgenic *Arabidopsis Pi21* lines (*pen2 NahG pmr5 mlo2* background) at 48 h post-inoculation (hpi) expressed as percentages of total infection sites. (c) Mean lengths of infection hyphae measured at 48 hpi. (d–g) Mean frequencies of infection site types in transgenic *Arabidopsis Pi21* lines (*pen2 NahG pmr5 mlo2* background) at 48 hpi expressed as percentages of penetrated cells. (d) Type I, (e) type II, (f) type III, (g) type IV. Cont., control *pen2 NahG pmr5 mlo2* plants; 4-1 and 5-1, two independent T_3 lines (*pen2 NahG pmr5 mlo2* background). Values are means ± standard errors ($n = 3$). Bars sharing the same lowercase letters are not significantly different (Tukey's highly significant differences test; $P \geq 0.05$, $n = 3$).

preferentially stimulated hyphal branching, and AGB1 restricted both hyphal elongation and branching. Although detected no effect of *pmr5* on post-penetration resistance in *pen2 NahG pmr5* and *pen2 pmr5 agb1* plants (Fig. 1d–g), *pen2 NahG pmr5 agb1* plants had significantly higher frequencies of branched hypha establishment than other mutants (Fig. 1g). Because PMR5 inhibited hyphal elongation and AGB1 restricted hyphal elongation and branching, *agb1* likely had synergistic effects on hyphal branch formation in the *pen2 NahG pmr5* background. The *mlo2* mutation enhanced hyphal length and significantly increased the rate of infection hypha branch formation in the *pen2 pmr5* background (Fig. 2b, f), which suggests that MLO2 restricted both hyphal elongation and branching in this background.

Rice *pi21* is a recessive gene conferring durable resistance to blast disease. Wild-type Pi21 appears to slow host defense responses, suggesting that Pi21 may promote fungal growth in plants[19]. We determined whether rice Pi21 would support fungal growth in non-host *Arabidopsis*. In transgenic *Pi21* lines in *pen2* and *pen2 NahG pmr5 mlo2* backgrounds, rice Pi21 did not affect *Arabidopsis* penetration resistance (Fig. 3b and Supplementary Fig. S5a). However, although rice Pi21 significantly enhanced hyphal elongation and hyphal movement from penetrated epidermal cells to adjacent mesophyll cells in the *pen2 NahG pmr5 mlo2* background (Figs. 3c and 4f), this was not the case in the *pen2* background (Supplementary Figs. S5b and S7). Hence, rice Pi21 regulated hyphal elongation and movement, but not penetration defense, in *Arabidopsis*. Factors other than Pi21 may have affected hyphal movement from penetrated epidermal cells to adjacent epidermal cells. Rice Pi21 contains putative protein–protein interaction motifs[19], which suggests that Pi21 interacting factors occur in *Arabidopsis*. Rice Pi21 also contains a heavy metal–transport/detoxification protein domain. Yeast copper chaperone ATX1 represents the proteins containing this domain[20]. Although homologs of yeast *ATX1* are present in *Arabidopsis*, rice *Pi21* (Os04g0401000) belongs to a group of genes that are distinct from these homologs[19], suggesting that *Pi21*, which is a gene for susceptibility to *M. oryzae*, occurs in rice but not in *Arabidopsis*. Hence, *Pi21* may predispose rice to blast disease.

PEN2, PMR5, AGB1, and MLO2 functioned in both penetration and post-penetration resistance. Moreover, epistasis occurred among these genes at both levels of resistance. Elevated fungal entry rates were related to fungal growth rates in penetrated cells (Figs. 1, 2 and Supplementary Figs. S1, S2). Therefore, penetration and post-penetration resistance in *Arabidopsis* likely share a common mechanism. Indeed, PEN2 and PEN3 function in both penetration and post-penetration resistance in *Arabidopsis*–powdery mildew interactions[10,11]. PEN2 converts a nontoxic substrate into a toxic product, which is then exported either directly or following further modification to the apoplast by PEN3; the toxic product poisons the fungal penetration peg as it attempts to breach the cell wall[11]. Post-penetration roles of PEN2 and PEN3 may therefore have involved PEN3 toxin export to the extrahaustorial matrix, where the haustorium was poisoned; this would have limited the initiation and growth of secondary fungal hyphae. Therefore, PEN2 in *Arabidopsis* likely operated by poisoning fungal penetration (i) as penetration pegs passed through the cell wall and (ii) when infection hyphae invaded the plasma membrane.

Silencing of the arbuscular mycorrhizal (AM) symbiosis-induced gene *Vapyrin* impairs epidermal penetration by AM fungi and prevents arbuscule formation in *Medicago truncatula*[21]. The phenotypes of *Vapyrin*-silencing plants indicate that a common cellular mechanism may be required to enable hyphal growth through epidermal cells and arbuscule development in cortical cells[21]. Vapyrin may play a role in cellular remodeling processes that support entry, possibly those that facilitate membrane invagination[21]. In compatible rice–*M. oryzae* interactions, primary hyphae and then bulbous invasive hyphae penetrate living rice cells while separating host cytoplasm from host extracellular space with a plant-derived extra-invasive hyphal membrane (EIHM)[2]. Moreover, infection hyphae are established in host-adapted and non-adapted *Colletotrichum* species through invagination of the host plasma membrane[22]. Considering these diverse lines of evidence, we suggest that establishment of infection hyphae through invagination of the host plasma membrane is a common mechanism of fungal penetration into plant cells. We also suggest that PMR5, AGB1, and MLO2 are involved in the invagination process. These factors function in plant cell membranes; PMR5 likely targets the endoplasmic reticulum (ER)[23], AGB1 is localized in both the plasma membrane and the ER[24], and MLO is localized in the plasma membrane[25].

The fungus never sporulated in any of the multiple mutants we tested (including *Pi21* transgenic lines), indicating that post-penetration resistance to *M. oryzae* was effective in *Arabidopsis*. Therefore, additional and currently unidentified genes probably had roles in *Arabidopsis* post-penetration resistance to *M. oryzae*. Alternatively, essential requirements needed to establish the pathogen's biotrophic stage may be absent in *Arabidopsis*. NHR may now be considered as the consequence of ineffective microbial effectors with no suppression of pathogen-associated molecular pattern (PAMP)-triggered immunity (PTI) and/or effector-triggered immunity (ETI)[26]. Alternatively, (individual) effectors may not have been selected to evade recognition; they would thus be recognized in non-host plants, resulting in ETI. Adapted pathogens might conceivably use effector molecule transfer to interfere with both penetration and post-penetration defense mechanisms and to establish basic compatibility. Studies examining the functions of blast effectors in NHR of *Arabidopsis* are certainly warranted.

Here, we have presented the interaction between *Arabidopsis* and *M. oryzae* as a model system for dissecting NHR mechanisms. Correlated genetic analysis and cytological investigation allowed us to characterize genes involved in several steps of *Arabidopsis* NHR to *M. oryzae*. This work will contribute to improved and durable disease resistance in important crops.

Methods

Plant material. *Arabidopsis* plants were grown under short-day conditions (9:15 L:D) at 22°C in a growth room. The *Arabidopsis* accession code was Col-0. We used the following mutants and transgenic plants: *pen2-1*[10], *pmr5-1*[27], *agb1-2*[28], *Atmlo2-7* (SALK_079850), and *NahG* (all with the Col-0 background)[29]. These mutants were used for crosses. Respective multiple mutants were identified in F_2 progeny by polymerase chain reaction (PCR) using suitable CAPS or derived CAPS (dCAPS) markers; genotypes were verified in the subsequent (F_3) generation.

Transgenic *Arabidopsis* lines overexpressing rice *Pi21* cDNA. A cDNA containing the susceptible *Pi21* allele from Nipponbare (AK070581) was digested with *Sfi*I and cloned into the *Sfi*I sites of the binary vector pBIG2113SF[30]. *Arabidopsis pen2*, *pen2 NahG pmr5 agb1*, and *pen2 NahG pmr5 mlo2* plants were transformed with the resulting construct by floral dipping[31], and primary transformants (T_1 generation) were selected on hygromycin in tissue culture. Progeny of T_2 lines (T_3 generation) were used for *M. oryzae* inoculations. RNA samples were prepared from the T_3 lines. Reverse transcription (RT)-PCR was performed for *Pi21* and *actin* using the following oligonucleotide primers: Pi21-F, CGGCAAATTTGACAGATGGGTAT; Pi21-R, CTTCTCCGGGTCGAACTTC; Actin-F, GTTGGGATGAACCAGAAGGA; and Actin-R, GACCACCGATCCAGACACT. Genomic DNA of *Arabidopsis* accession Col-0 served as the control template for distinguishing cDNA and genomic DNA–derived PCR products.

Fungal material. *M. oryzae* isolate Kita 1 (race 007) was incubated on oatmeal agar media in Petri dishes at 25°C; the inoculum was prepared as previously described[32]. To inoculate *M. oryzae*, 15-µl droplets (10^4 spores/ml) were applied to leaves of 4–5-week-old plants, which were then kept in conditions of saturating humidity until harvested.

Cytology and quantification of fungal growth. Infected leaves were harvested at the time point indicated. After cutting, the leaves were submerged directly in ethanolic lactophenol solution and were heated to 90°C for 3 min. The leaf samples were cooled to room temperature for 10 min and were subsequently incubated in saturated chloral hydrate (2.5 g/ml) for 2 days. To quantify cell entry and fungal growth, we examined the germinated fungal sporelings that developed appressoria on six leaves from six independent plants per experiment and genotype (minimum of 100 appressoria/leaf evaluated). Penetration success of *M. oryzae* was detected by the

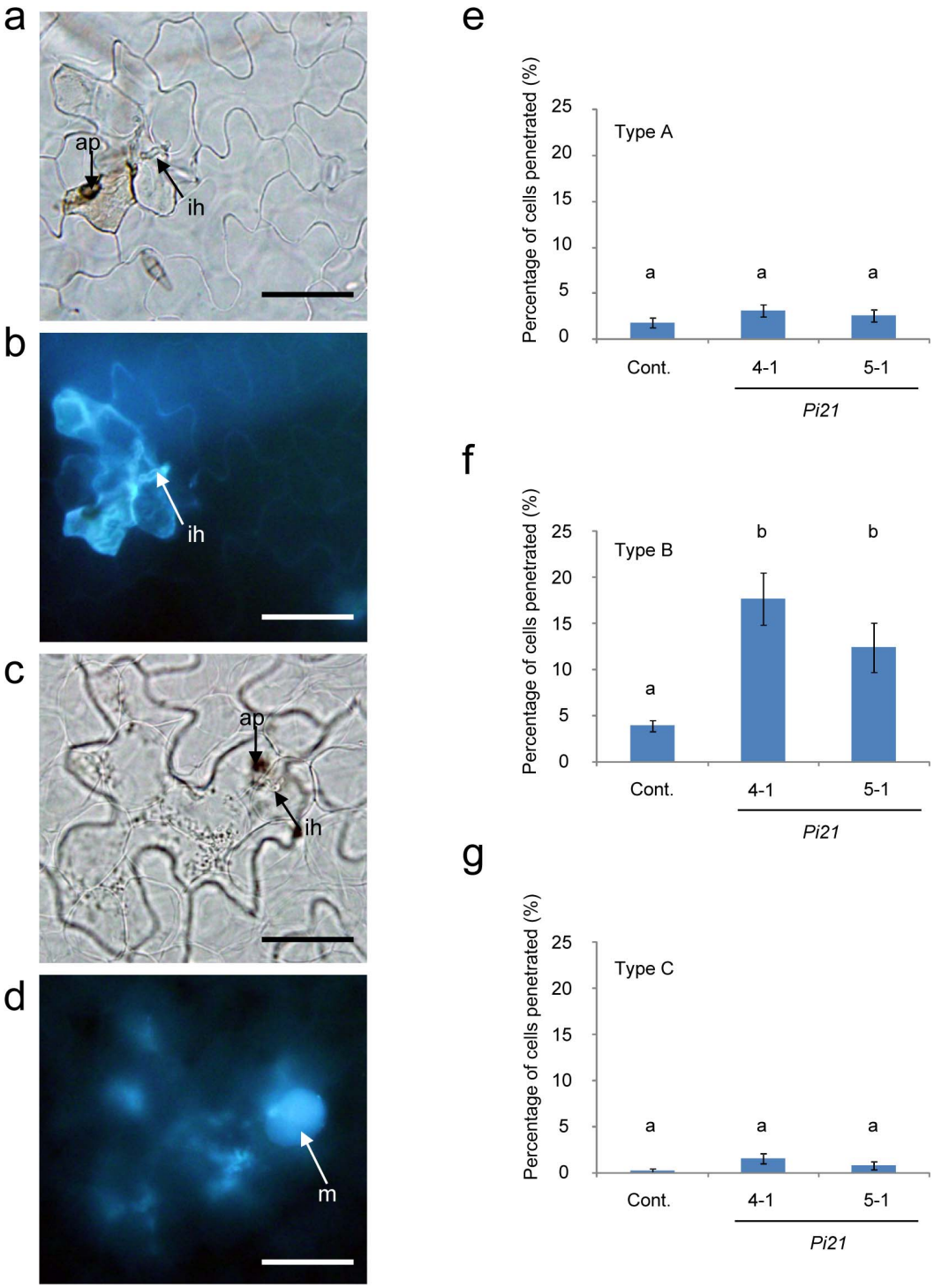

Figure 4 | Movement of infection hyphae from penetrated epidermal cells to adjacent cells in transgenic *Arabidopsis Pi21* lines. Microscopic view of infection sites in transgenic *Arabidopsis Pi21* lines (*pen2 NahG pmr5 mlo2* background). (a) Movement of infection hyphae from a penetrated epidermal cell to an adjacent epidermal cell in transgenic *Arabidopsis Pi21* lines (*pen2 NahG pmr5 mlo2* background). The infection site was photographed at 48 h post-inoculation (hpi). The first invaded epidermal cell was associated with slight browning. ap, appressorium; ih, infection hyphae in adjacent epidermal cell. Bars = 50 µm. (b) Fluorescence microscopic view of the infection site of (a). ih, infection hyphae in adjacent epidermal cell. Bars = 50 µm. (c) Movement of infection hyphae from a penetrated epidermal cell to adjacent mesophyll cells in transgenic *Arabidopsis Pi21* lines (*pen2 NahG pmr5 mlo2* background). The infection site was photographed with the mesophyll cells in focus (48 hpi). ap, appressorium; ih, infection hyphae in adjacent mesophyll cell. Bars = 50 µm. (d) Fluorescence microscopic view of the infection site in (c). m, penetrated adjacent mesophyll cell. Bars = 50 µm. (e–g) Cell–cell movements of infection hyphae were grouped into categories (A–C): A, hyphal movement from penetrated epidermal cell to adjacent epidermal cell; B, hyphal movement from penetrated epidermal cell to adjacent mesophyll cell; C, hyphal movement from penetrated epidermal cell to adjacent epidermal and mesophyll cells. Mean frequencies of various types of infection site in transgenic *Arabidopsis Pi21* lines (*pen2 NahG pmr5 mlo2* background) at 48 hpi expressed as percentages of penetrated cells. (e) Type A, (f) type B, (g) type C. Cont., control *pen2 NahG pmr5 mlo2* plants; 4-1 and 5-1, two independent T_3 lines (*pen2 NahG pmr5 mlo2* background). Values are means ± standard errors, $n = 3$ independent experiments. Bars sharing the same lowercase letters are not significantly different (Tukey's highly significant differences test; $P \geq 0.05$, $n = 3$).

occurrence of autofluorescence or hyphal elongation at infection sites using fluorescence and bright-field microscopy (BX51; OLYMPUS). Fluorescence was examined under a microscope with a mirror unit (U-MWIB3; OLYMPUS; excitation, 460–495 nm; dichroic, 505 nm; emission, 510 nm). The images were recorded with a digital camera (DP72; OLYMPUS). Length and branch formation of infection hyphae at infection sites were also examined by bright-field microscopy. Cell entry and fungal growth on each plant genotype were quantified in at least three independent experiments.

Data collection and analysis. Data were collected from six leaves from six independent plants per line. A minimum of 100 infection sites were inspected per leaf. Data were compared using Tukey's highly significant difference (HSD) tests. Calculations were performed on three data sets ($n = 3$) and $P < 0.05$ indicated statistically significant effects.

1. Koga, H. in *Major Fungal Diseases of Rice Recent Advances* 87–110 (Kluwer Academic Publishers, 2001).
2. Kankanala, P., Czymmek, K. & Valent, B. Roles for rice membrane dynamics and plasmodesmata during biotrophic invasion by the blast fungus. *Plant Cell* **19**, 706–724 (2007).
3. Wilson, R. A. & Talbot, N. J. Under pressure: investigating the biology of plant infection by *Magnaporthe oryzae*. *Nat Rev Microbiol* **7**, 185–195 (2009).
4. Dean, R. A. *et al*. The genome sequence of the rice blast fungus *Magnaporthe grisea*. *Nature* **434**, 980–986 (2005).
5. Ebbole, D. J. *Magnaporthe* as a model for understanding host-pathogen interactions. *Annu Rev Phytopathol* **45**, 437–456 (2007).
6. Howard, R. J., Ferrari, M. A., Roach, D. H. & Money, N. P. Penetration of hard substrates by a fungus employing enormous turgor pressures. *Proc Natl Acad Sci USA* **88**, 11281–11284 (1991).
7. Lipka, U., Fuchs, R. & Lipka, V. *Arabidopsis* non-host resistance to powdery mildews. *Curr Opin Plant Biol* **11**, 404–411 (2008).
8. Heath, M. C. Nonhost resistance and nonspecific plant defenses. *Curr Opin Plant Biol* **3**, 315–319 (2000).
9. Collins, N. C. *et al*. SNARE-protein-mediated disease resistance at the plant cell wall. *Nature* **425**, 973–977 (2003).
10. Lipka, V. *et al*. Pre- and postinvasion defenses both contribute to nonhost resistance in *Arabidopsis*. *Science* **310**, 1180–1183 (2005).
11. Stein, M. *et al*. *Arabidopsis* PEN3/PDR8, an ATP binding cassette transporter, contributes to nonhost resistance to inappropriate pathogens that enter by direct penetration. *Plant Cell* **18**, 731–746 (2006).
12. Kobae, Y. *et al*. Loss of AtPDR8, a plasma membrane ABC transporter of *Arabidopsis thaliana*, causes hypersensitive cell death upon pathogen infection. *Plant Cell Physiol* **47**, 309–318 (2006).
13. Bednarek, P. *et al*. A glucosinolate metabolism pathway in living plant cells mediates broad-spectrum antifungal defense. *Science* **323**, 101–106 (2009).
14. Clay, N. K., Adio, A. M., Denoux, C., Jander, G. & Ausubel, F. M. Glucosinolate metabolites required for an *Arabidopsis* innate immune response. *Science* **323**, 95–101 (2009).
15. Maeda, K. *et al*. AGB1 and PMR5 contribute to PEN2-mediated preinvasion resistance to *Magnaporthe oryzae* in *Arabidopsis thaliana*. *Mol Plant-Microbe Interact* **22**, 1331–1340 (2009).
16. Maeda, K. *et al*. Nonhost resistance to *Magnaporthe oryzae* in *Arabidopsis thaliana*. *Plant Signal Behav* **5**, 755–756 (2010).
17. Schreiber, C., Slusarenko, A. J. & Schaffrath, U. Organ identity and environmental conditions determine the effectiveness of nonhost resistance in the interaction between *Arabidopsis thaliana* and *Magnaporthe oryzae*. *Mol Plant Pathol* **12**, 397–402 (2011).
18. Jarosch, B., Jansen, M. & Schaffrath, U. The ambivalence of the barley Mlo locus: Mutations conferring resistance against powdery mildew (*Blumeria graminis* f. sp. hordei) enhance susceptibility to the rice blast fungus *Magnaporthe grisea*. *Molecular Plant-Microbe Interactions* **6**, 508–514 (1999).
19. Fukuoka, S. *et al*. Loss of function of a proline-containing protein confers durable disease resistance in rice. *Science* **325**, 998–1001 (2009).
20. Lin, S. J. & Culotta, V. C. The ATX1 gene of *Saccharomyces cerevisiae* encodes a small metal homeostasis factor that protects cells against reactive oxygen toxicity. *Proc Natl Acad Sci USA* **92**, 3784–3788 (1995).
21. Pumplin, N. *et al*. *Medicago truncatula* Vapyrin is a novel protein required for arbuscular mycorrhizal symbiosis. *Plant J* **61**, 482–494 (2010).
22. Hiruma, K. *et al*. Entry mode-dependent function of an indole glucosinolate pathway in *Arabidopsis* for nonhost resistance against anthracnose pathogens. *Plant Cell* **22**, 2429–2443 (2010).
23. Vogel, J. P., Raab, T. K., Somerville, C. R. & Somerville, S. C. Mutations in PMR5 result in powdery mildew resistance and altered cell wall composition. *Plant J* **40**, 968–978 (2004).
24. Wang, S., Narendra, S. & Fedoroff, N. Heterotrimeric G protein signaling in the *Arabidopsis* unfolded protein response. *Proc Natl Acad Sci USA* **104**, 3817–3822 (2007).
25. Bhat, R. A., Miklis, M., Schmelzer, E., Schulze-Lefert, P. & Panstruga, R. Recruitment and interaction dynamics of plant penetration resistance components in a plasma membrane microdomain. *Proc Natl Acad Sci USA* **102**, 3135–3140 (2005).
26. Jones, J. D. & Dangl, J. L. The plant immune system. *Nature* **444**, 323–329 (2006).
27. Vogel, J. & Somerville, S. Isolation and characterization of powdery mildew-resistant *Arabidopsis* mutants. *Proc Natl Acad Sci USA* **97**, 1897–1902 (2000).
28. Chen, J. G., Gao, Y. & Jones, A. M. Differential roles of *Arabidopsis* heterotrimeric G-protein subunits in modulating cell division in roots. *Plant Physiol* **141**, 887–897 (2006).
29. Lawton, K. *et al*. Systemic acquired resistance in Arabidopsis requires salicylic acid but not ethylene. *Mol Plant-Microbe Interact* **8**, 863–870 (1995).
30. Ichikawa, T. *et al*. The FOX hunting system: an alternative gain-of-function gene hunting technique. *Plant J* **48**, 974–985 (2006).
31. Clough, S. J. & Bent, A. F. Floral dip: a simplified method for *Agrobacterium*-mediated transformation of *Arabidopsis thaliana*. *Plant J* **16**, 735–743 (1998).
32. Koga, H. & Nakayachi, O. Morphological studies on attachment of spores of Magnaporthe grisea to the leaf surface of rice. *J Gen Plant Pathol* **70**, 11–15 (2004).

Acknowledgments

We would like to acknowledge ARBC for providing seeds of Col-0, *agb1-2*, and *Atmlo2-7*, and the Rice Genome Resource Center (National Institute of Agrobiological Sciences, Japan) for providing *Pi21* cDNA. We thank H. Koga (Ishikawa Prefectural University) for providing the *M. oryzae* isolate, P. Schulze-Lefert (Max Planck Institute for Plant Breeding Research) for seeds of *pen2-1*, Syngenta for *NahG*, J. Vogel (United States Department of Agriculture) for *pmr5-1*, and Y. Kondou (RIKEN) for the binary vector. This work was supported by a grant-in-aid for scientific research at Fukui Prefectural University to A.I. from Fukui Prefecture, Japan.

Author contrications

M.N., R.N., K.K., and R.I. performed experiments. A.I. designed experiments, interpreted results and wrote the manuscript.

Additional information

Supplementary information accompanies this paper at http://www.nature.com/scientificreports

Competing financial interests: The authors declare no competing financial interests.

How to cite this article: Nakao, M., Nakamura, R., Kita, K., Inukai, R. & Ishikawa, A. Non-host resistance to penetration and hyphal growth of *Magnaporthe oryzae* in *Arabidopsis*. *Sci. Rep.* **1**, 171; DOI:10.1038/srep00171 (2011).